halogen in two stages, whereby ~80% of the halogen is easily lost from the tetragonal structure below 200 °C and the remaining halogen is lost immediately after the tetragonal–orthorhombic phase change. This leaves M(HDPG)$_2$ and an impurity phase which causes a depression of the melting point. The iodine-containing complexes also lost halogen in two separate processes; however, in contrast to the bromine-containing complexes, there was no obvious correlation with the phase change. The loss of halogen from the mixed halogen-containing species is more complex than that observed for the M(HDPG)$_2$X, (M = N, Pd; X = Br, I). Preliminary kinetic data is consistent with a one-dimensional diffusion model for the halogen loss from these complexes.

Acknowledgment. We wish to thank Mr. E. C. Williams and J. W. Lewicki, and G. Fekete for technical assistance in the performance of several experiments. We also wish to thank Professor T. J. Marks (Northwestern) for obtaining Raman spectra.

Supplementary Material Available: Tables of elemental analyses (Tables I–IV) (4 pages). Ordering information is given on any current masthead page.

References and Notes

(1) J. S. Miller and A. J. Epstein, *Prog. Inorg. Chem.*, **20**, 1 (1976), and references cited therein.
(2) J. S. Miller, *Adv. Chem. Ser.*, **No. 150**, 18 (1976).
(3) H. J. Keller, Ed., *NATO Adv. Study Inst., Ser. B*, **7**, 1 (1975).
(4) L. V. Interrante, Ed., *ACS Symp. Ser.*, **No. 5**, 1 (1975).
(5) H. G. Schuster, Ed., *Lect. Notes Phys.*, **34**, 1 (1975).
(6) T. W. Thomas and A. E. Underhill, *Chem. Soc. Rev.*, 1, 99 (1972).
(7) K. Krogmann, *Angew. Chem., Int. Ed. Engl.*, **8**, 35 (1969).
(8) I. F. Shchegolev, *Phys. Status Solidi A*, **12**, 9 (1972).
(9) H. R. Zeller, *Festkörperprobleme*, **13**, 31 (1973).
(10) L. E. Edelman, *J. Am. Chem. Soc.*, **72**, 5765 (1950).
(11) A. S. Foust and R. H. Soderberg, *J. Am. Chem. Soc.*, **89**, 5507 (1967).
(12) H. J. Keller and K. Seibold, *J. Am. Chem. Soc.*, **93**, 1309 (1971).
(13) N. S. Garif'yanov, I. I. Kalinichenko, I. V. Ovchinnikov, and Z. F. Martyanova, *Dokl. Chem.*, **17B**, 795 (1967).
(14) J. S. Miller and S. Z. Goldberg, *Inorg. Chem.*, **14**, 2294 (1975).
(15) H. Gleizes, T. J. Marks, and J. A. Ibers, *J. Am. Chem. Soc.*, **97**, 3545 (1975); T. J. Marks, D. F. Webster, S. L. Ruby, and S. Schultz, *J. Chem. Soc., Chem. Commun.*, in press; H. Endres, H. J. Keller, M. Mégnamisi-Bélombé, W. Moroni, H. Pritzkow, J. Weiss, and R. Cómes, *Acta Crystallogr.*, in press.
(16) Diffuse x-ray scattering of the iodine oxidation product with Ni($C_6H_5N_2O_2$)$_2$ could only account for a one-dimensional array of halides;[17] thus the previously suggested pentacoordinate structure for Ni(HDPG)$_2$Br[13] is erroneous.
(17) H. Endres, H. J. Keller, and R. Lehmann, *Inorg. Nucl. Chem. Lett.*, 11, 769 (1975).
(18) A. E. Underhill, D. M. Watkins, and R. Pethig, *Inorg. Nucl. Chem. Lett.*, **9**, 1269 (1973).
(19) O. Glemser in "Handbook for Preparative Inorganic Chemistry", 2d ed, Vol. 1, G. Brauer, Ed., R. F. Riley, Translator, Academic Press, New York, N.Y., 1962, p 67.
(20) J. S. Miller and A. O. Goedde, *J. Chem. Educ.*, **50**, 431 (1973).
(21) J. S. Miller, S. H. Kravitz, and S. Kirschner, Abstracts, 155th National Meeting of the American Chemical Society, San Francisco, Calif., March 1968, No. B-45; manuscript in preparation.
(22) R. D. Gillard and G. Wilkinson, *J. Chem. Soc.*, 6041 (1963).
(23) The oxidation potentials increase as Br_2(1.065 V) > $(SCN)_2$ (0.77 V) > I_2(0.536 V). J. P. Jesson and E. L. Muetterties, "Chemist's Guide", Marcel Dekker, Inc., New York, N.Y., 1969, pp 9–10.
(24) Similar structures are observed for iodine oxidation product with Pd($C_2H_3N_2O_2$)$_2$[17,25] and Ni($C_6H_5N_2O_2$)$_2$.[26-28]
(25) H. Endres, H. J. Keller, R. Lehmann, and J. Weiss, *Acta Crystallogr., Sect. B*, **32**, 627 (1975).
(26) H. J. Keller, *NATO Adv. Study Inst.*, Ser. B, **7**, 315 (1975) (see ref 3).
(27) H. Endres, H. J. Keller, M. Megnamisi-Bélombé, W. Moroni, and D. Nöthe, *Inorg. Nucl. Chem. Lett.*, **10**, 467 (1974).
(28) H. Endres, H. J. Keller, W. Moroni, and J. Weiss, *Acta Crystallogr., Sect. B*, **31**, 2357 (1975); H. Endres, H. J. Keller, M. Megnamisi-Bélombé, W. Moroni, H. Prinzkow, J. Weiss, and R. Comés, submitted for publication.
(29) For a 1:1 X/M ratio.
(30) (a) T. J. Marks, private communication; (b) J. L. Petersen, C. J. Schramm, D. R. Stojakovic, B. M. Hoffman, and T. J. Marks, submitted for publication; (c) B. M. Hoffman, Abstracts, Pacific Conference on Chemistry and Spectroscopy, Oct 1975, No. 177.
(31) F. A. Cotton and G. Wilkinson, "Advanced Inorganic Chemistry", 3d ed, Wiley, New York, N.Y., 1972, p 483.
(32) Recently thiocyanogen oxidation of tetrathiofulvalene has been reported to yield a nonstoichiometric complex with the pseudohalide filling a channel parallel to the *c* axis.[33]
(33) F. Wudl, *J. Am. Chem. Soc.*, **97**, 1962 (1975); abstracts, Pacific Conference on Chemistry and Spectroscopy, Oct 1975, No. 148.
(34) R. J. Warmack, T. A. Callcott, and C. R. Watson, *Phys. Rev. B*, **12**, 3336 (1975).
(35) R. B. Somano, A. Gupta, V. Hadek, T. Datta, M. Jones, R. Deck, and A. M. Hermann, *J. Chem. Phys.*, **63**, 4970 (1975).
(36) S. J. LaPlaca, P. W. R. Corfield, R. Thomas, and B. A. Scott, *Solid State Commun.*, 17, 635 (1975).
(37) J. J. Daly and F. Sanz, *Acta Crystallogr., Sect. B*, **31**, 620 (1975).
(38) C. K. Johnson and C. R. Watson, Jr., *J. Chem. Phys.*, in press.
(39) H. Scher, unpublished results

Electronic Structure of Three-Coordinate Nickel(I): Electron Paramagnetic Resonance of Nickel-Doped Halobis(triphenylphosphine)copper(I)

Mark J. Nilges, E. Kent Barefield, R. Linn Belford,*[1] and Phillip H. Davis

Contribution from the Department of Chemistry, University of Illinois, Urbana, Illinois 61801. *Received August 11, 1976*

Abstract: Successful preparation and electron paramagnetic resonance of single crystals of Ni-doped $(Ph_3P)_2CuX{\cdot}0.5C_6H_6$ (X = Cl, Br) are described. For both the chloro and bromo complexes the isotropic and anisotropic parts of the ^{31}P superhyperfine tensors of the two inequivalent phosphorus ligands are markedly different. Additional superhyperfine structure observed in the spectra of the bromo complex is attributed to $^{79,81}Br$ superhyperfine and nuclear quadrupole coupling. Anisotropic line widths in the chloro complex are attributed to unresolved $^{35,37}Cl$ superhyperfine and quadrupole structure. The orientations and magnitudes of the various EPR tensors, including the Br quadrupole coupling, suggest that the metal–halogen bond is fairly ionic (~80%), and that the unpaired spin is rather strongly localized on the Ni atom yet is involved in a halogen–metal $p_\pi \rightarrow d_{xy}$ bond.

Although complexes containing nickel in the +1 oxidation state are still rather uncommon, the number of examples is steadily increasing.[2] There is also clear evidence that certain of these complexes represent thermodynamically stable species; i.e., there are no kinetic barriers to disproportionation to the more normal 0 and +2 oxidation states. Halotris(triphenylphosphine)nickel(I) complexes are excellent examples of this type of system. In 1964, Heimbach reported these complexes as the products of the following reactions:[3]

$$(Ph_3P)_4Ni + (Ph_3P)_2NiX_2 \rightarrow 2(Ph_3P)_3NiX$$

$$[(allyl)NiX]_2 + 6Ph_3P \rightarrow 2(Ph_3P)_3NiX + hexadiene$$

$$(Ph_3P)_4Ni + \tfrac{1}{2}X_2 \rightarrow (Ph_3P)_3NiX + Ph_3P$$

Cryoscopic molecular weight measurements indicated that these complexes were extensively dissociated in benzene solution. Although the products of dissociation were not clearly established, Heimbach also prepared bisphosphine complexes by the reaction:

$$(Ph_3P)_2Ni(C_2H_4) + (Ph_3P)_2NiX_2 \rightarrow 2(Ph_3P)_2NiX + C_2H_4$$

These complexes were monomeric in benzene by cryoscopy. In 1967, Porri et al.[4] rediscovered the trisphosphine complexes and also found that they were dissociated in benzene. Since then, the bis- or trisphosphine complexes have been isolated as products of nickel(0) or nickel(II) reactions no less than eight times.[5-11] In particular, they have been obtained as products of homolytic cleavage of nickel–carbon bonds in several alkyl complexes.[9-11] These complexes have also been implicated as catalysts or catalyst precursors for olefin isomerization.[7,12,13] Analogous complexes with other phosphine ligands have been less extensively studied but tristriethylphosphine[6,14,15] and tristributylphosphine[15] examples have been prepared.

The work presented in this paper is a result of our interests in both the chemistry of unusual oxidation states of nickel and the applications of electron paramagnetic resonance spectroscopy to chemical problems. In spite of the frequency with which the halotriphenylphosphine–nickel(I) complexes have been observed, very little is known in detail about their solution equilibria or their electronic structures. Since monomeric nickel(I) species must be paramagnetic $S = \tfrac{1}{2}$ systems, they should be amenable to study by EPR. In principle, EPR spectroscopy could provide information about the composition of species present in solution in the case of the phosphine complexes since ^{31}P superhyperfine (shf) interactions are expected to be substantial and the hyperfine pattern should be predictable. Heimbach[3] reported that EPR spectra typical of $S = \tfrac{1}{2}$ systems were exhibited by the nickel(I) complexes which he prepared, but gave no spectra or data. Furthermore, single-crystal EPR studies could provide exact information regarding Zeeman and phosphorus shf tensor anisotropy and in ideal cases the nature of the ground state electronic structure of the complex. Shf interaction with the halide ligand, if observable, would considerably strengthen our knowledge of the bonding.

When we first attempted to use EPR as a means of examining the $(Ph_3P)_nNiX$ species the results were very disappointing. Fluid solutions exhibited only a single broad line regardless of conditions (solvent, excess phosphine, temperature, etc.), and spectra of their frozen solutions were too poorly resolved for interpretation. Likewise, spectra obtained on polycrystalline samples were rich in structure, but too poorly resolved for clear-cut interpretation. In order to resolve some of the questions raised by these measurements, we have undertaken single-crystal EPR studies of certain of the halophosphine–nickel(I) complexes. This paper concerns EPR studies of single crystals of $(Ph_3P)_2NiX$ (X = Cl, Br) doped into the corresponding copper(I) host. The x-ray structure determination of the $(Ph_3P)_2CuBr{\cdot}0.5C_6H_6$, done in preparation for this work, was described earlier.[16]

Experimental Section

The synthesis of chloro- and bromotris(triphenylphosphine)nickel(I) has previously been described.[3] Chloro- and bromobis(triphenylphosphine)copper(I) were synthesized according to the method outlined by Davis et al.[16] In addition to the 2:1 triphenylphosphine–copper complexes, the 3:1, 3:2, and 1:1 complexes could be obtained by adjusting the solvents and the amount of excess triphenylphosphine present during recrystallization of the bis complexes.

Nickel-doped single crystals of the halobis(triphenylphosphine) copper hemibenzate complexes grew from a 2:3 mixture of cyclohexane and benzene in which was dissolved ~20 mole % triphenylphosphine and 1 mole % of the appropriate tris nickel complex. (The tris complexes, as mentioned above, dissociate to the bis form in benzene.) Slow evaporation of the solutions under their own atmosphere yielded well-formed crystals after 1 week.

Single-crystal, powder, and frozen solution spectra were recorded at X-band and Q-band frequencies with Varian E-9 and E-15 spectrometers, respectively. The magnetic field was calibrated by proton resonance. The Q-band frequency was determined by the observation of the electron resonance of powdered DPPH ($g = 2.0036$); the X-band frequency was determined with a digital frequency meter.

Crystals were mounted on an x-ray goniometer head, and a well-formed face of a crystal was aligned by means of an optical goniometer. With the aid of the known crystal structure and morphology a selected molecular axis could be aligned with the rotation axis of the EPR goniometer by adjustment of the two arcs of the x-ray goniometer head. In addition, spectra could be obtained for the magnetic field parallel to the principal directions of the electronic Zeeman tensor through the use of a double rotating goniometer. The samples were held at liquid nitrogen temperature for all measurements.

Spectra of the bromo complex were fitted to the following spin Hamiltonian:

$$\mathcal{H} = \mu_B B{\cdot}g{\cdot}S + S{\cdot}A^{Br}{\cdot}I^{Br} + I^{Br}{\cdot}Q^{Br}{\cdot}I^{Br} - \mu_N B{\cdot}g_N{\cdot}I^{Br} + \sum_{i=1}^{2} S{\cdot}A^{P_i}{\cdot}I^{P_i}$$

(The halogen shf and quadrupole terms were dropped for the chloro complex as no structure from these terms could be resolved.) The computer programs for interpreting the spectra of the bromo complex used 8 × 8 matrix diagonalization to compute energies for the first four terms of the above Hamiltonian and second-order perturbation for the phosphorus shf splittings. Because the splitting due to the two natural occurring isotopes of bromine was not observed, the average nuclear moments and coupling constants were used. The bromine quadrupole and shf tensors and all out-of-plane tensor components were assumed collinear.

Results and Analysis

Because the naturally occurring isotope of nickel, ^{61}Ni, is only 1.19% abundant, the spectra revealed no nickel hyperfine structure.

Superhyperfine structure (shfs) in both single-crystal and powder EPR spectra of nickel-doped $(Ph_3P)_2CuBr{\cdot}0.5C_6H_6$ is complicated, highly orientation dependent, and asymmetric. The intensities of the satellite lines, which can be seen in the shfs in Figure 1, range from near zero to full intensity (i.e., as strong as the main lines). On the other hand, shfs for nickel-doped $(Ph_3P)_2CuCl{\cdot}0.5C_6H_6$ consists of four broad lines, which we attribute to splitting by the two ^{31}P ($I = \tfrac{1}{2}$) nuclei in the complex.

One source of complication, seen in some instances,[17a] is a nuclear quadrupole interaction competitive with hyperfine splittings. We believe that the extra shfs seen in the bromo complex is due to the coupling of the electron spin with the magnetic moment of the two naturally occurring isotopes of bromine, ^{79}Br and ^{81}Br, and that the observed satellite lines are "forbidden" nuclear spin-flip transitions induced by the quadrupole moment of the bromine isotopes. Similar satellite lines have been observed in the EPR spectra of gold complexes[17b] in which the ^{197}Au quadrupole coupling constants are much larger than hyperfine coupling constants. The spectra

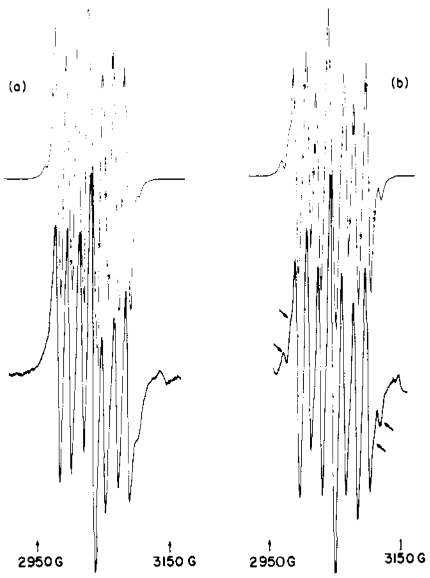

Figure 1. X-Band (9.1 GHz) EPR spectra for a nickel-doped single crystal of $(Ph_3P)_2CuBr{\cdot}0.5C_6H_6$ at orientations in the molecular xy plane: (a) 12° from the metal-bromine bond ($B\|g_2$) and (b) 20° from the metal-bromine bond. Upper curves are computer simulated; lower are experimental. Arrows point to the "forbidden" satellite lines.

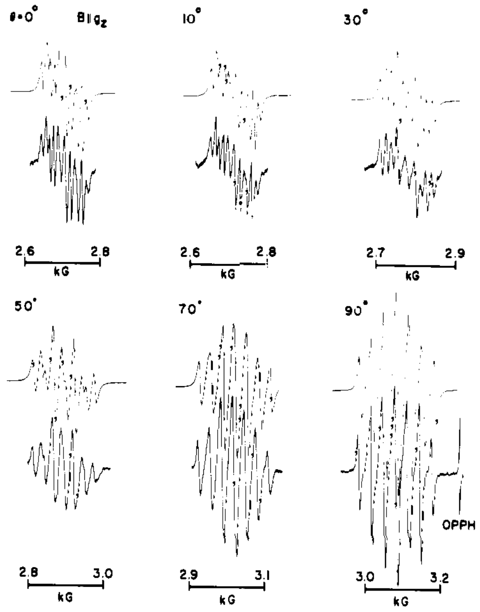

Figure 2. Angular dependence of X-band (9.1 GHz) EPR spectra for a nickel-doped single crystal of $(Ph_3P)_2CuBr{\cdot}0.5C_6H_6$ with B perpendicular to the metal-bromine bond. Upper curves are computer simulated; lower are experimental. The angle θ is with respect to the z axis of the molecule.

of these gold complexes also showed[17b] that the four "allowed" transitions expected for $I = {}^3\!/_2$ reduce to two or three lines at certain orientations. Thus, the unusual seven-line 1:1:1:2:1:1:1 pattern shown in Figure 1 can be explained: The four-line pattern seen in the shfs of the chloro complex is further split into doublets, not quartets, by the bromine nuclear spin.

Computer simulations showed that the unusual features in the shfs of the bromo complex can be accounted for if the largest principal component of the quadrupole tensor, Q_1, is directed along the nickel-bromine bond and is on the order of magnitude of the bromine shf splitting. The positions and intensities of the "forbidden" satellite lines relative to the "allowed" transitions are very sensitive to the magnitude of QD (${}^3\!/_2 Q_1$). Although it appeared that QD could be obtained to a high degree of precision, the task was not at all straightforward because ^{31}P and ^{79,81}Br shf coupling constants are also on the order of QD.

Fitting of the observed spectra was done by an iterative procedure that involved guessing reasonable values for shf and quadrupole coupling constants and adjusting them until a best fit was obtained. Initially, we assumed the principal components of the one ^{31}P shf tensor to be equal to those of the other ^{31}P shf tensor. Under this assumption, only very poor fits could be obtained and then only at certain orientations. Dropping this assumption, we arrived at reasonable fits (i.e., Figures 1, 2, and 3) and at shf and quadrupole coupling constants to within reasonable accuracy as reported in Table I. In simulation of observed spectra we also assumed the paramagnetic complex to have the same structure and orientation as the host and the in-plane shf principal axes to be directed parallel and perpendicular to the metal-ligand bonds. Although such assumptions must be suspect to some degree, they proved to be sufficient to permit rather good simulations of the observed spectra. Figure 4 shows the proposed assignments of the axes of the Zeeman and various shf tensors relative to the complex. As a check of the reliability of the single-crystal data reported for the bromo complex, we generated a simulated powder spectrum to compare with the experimental spectrum of the powdered dilute crystals; see Figure 5. The discernible noise between the out-of-plane features (leftmost and downfield) and the in-plane features is due to graining (i.e., a limited number of discrete crystallite orientations), which causes an incomplete cancellation of off-axis resonances.

The two ^{31}P shf tensors for the chloro complex are also inequivalent, and again we assumed the paramagnetic complex to have the same structure and orientation as its host. Principal components of the Zeeman and phosphorus shf tensor are reported in Table I. The inequivalency of the two ^{31}P shf tensors can be observed in the powder spectrum of the chloro complex shown in Figure 6. Instead of three lines with a 1:2:1 ratio as expected for two equivalent ^{31}P nuclei, four lines can be clearly seen in the out-of-plane portion of the spectrum.

Line widths for the chloro complex are anisotropic and could be fitted as follows:

$$w^2 = (g_1{}^2w_1{}^2l_1{}^2 + g_2{}^2w_2{}^2l_2{}^2 + g_3{}^2w_3{}^2l_3{}^2)/g^2$$

In addition, we found that the line widths for the chloro complex correlated well with the anisotropic bromine shf coupling of the bromo complex. Thus, we believe that the large line widths of the chloro complex are due to unresolved chlorine shf and quadrupole structure. Chlorine has two naturally occurring isotopes, both of which have smaller magnetic and quadrupole moments than the bromine isotopes.

The line widths of the bromo complex are also anisotropic, but in a different way than the chloro complex. Line widths along the principal directions of the Zeeman tensor are equal, yet they nearly double when the magnetic field is between principal directions of the Zeeman tensor. In addition, this off-axis broadening is more severe at Q-band than at X-band frequencies. Such an effect has been observed by other authors[18,19] and attributed to such things as crystal imperfection and vibration or distortion of the paramagnetic guest in the host. We took this effect into account when simulating spectra by adding an additional line width parameter equal to the slope of B_0 vs. orientation times a mean angle of libration or misorientation. Simulation showed this angle need be only 0.3°, and gave very good fits as shown in Figures 2 and 3.

Discussion

Bromine Nuclear Quadrupole Coupling. Although only the *relative* signs of the bromine shf and quadrupole coupling constants can be obtained from EPR spectra, the absolute signs

Table I. EPR Parameters for $(Ph_3P)_2NiX$ in $(Ph_3P)_2CuX{\cdot}0.5C_6H_6$ Host Lattices at 77 K[a,b]

	$(Ph_3P)_2NiCl$				$(Ph_3P)_2Ni^{79,81}Br$					
Axis	g	w (G)[d]	$A^{(P1)}$	$A^{(P2)}$	g	w (G)[d]	$A^{(P1)}$	$A^{(P2)}$	$A^{(Br)}$	$Q^{(Br)}$ [c]
1	2.111	15	67	41	2.112	6	72	35	−7	+5.7 (5)
2	2.167	9	55	39	2.209	6	53	35	+31	−3.3 (5)
3(z)	2.446	11	55	35	2.435	5	53	34	−14	−2.5 (5)
Av	2.241	12	59	38	2.252	6	59	35	3	0

[a] Uncertainties are ≤2 in the last digit unless a larger uncertainty is given in parentheses. [b] All shf and quadrupole coupling constants are in units of $10^{-4}\ cm^{-1}$. [c] Q_i (i = 1-3) = $eQeq_i/(2I(2I-1)) = \frac{1}{6}eQeq_i$ (for $I = \frac{3}{2}$), QD = $\frac{3}{2}Q_1 = \frac{1}{4}eQeq_1$ = 8.6 (5), QE = $\frac{1}{2}(Q_3 - Q_2)$ = 0.4 (3). [d] Line width (half-width at half-height).

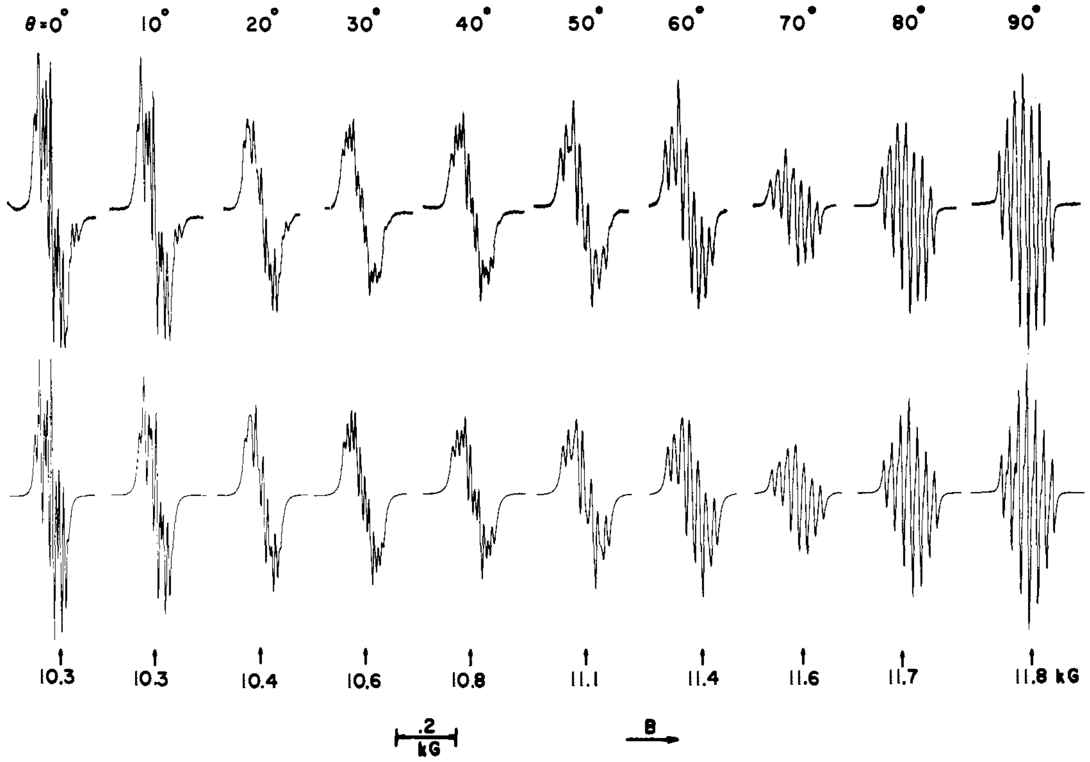

Figure 3. Angular dependence of Q-band (34.9 GHz) EPR spectra for a nickel-doped single crystal of $(Ph_3P)_2CuBr{\cdot}0.5C_6H_6$ with B perpendicular to the metal-bromine bond. Upper curves are experimental; lower are computer simulated. The angle θ is with respect to the z axis of the molecule. All spectra were run at the same instrument settings except that for θ = 70°, 80°, 90° the gain was reduced by a factor of 2.

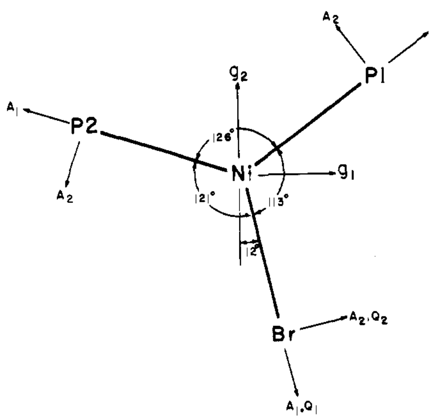

Figure 4. Principal axis directions of in-plane Zeeman, shf, and quadrupole tensor components in nickel-doped $(Ph_3P)_2CuBr{\cdot}0.5C_6H_6$.

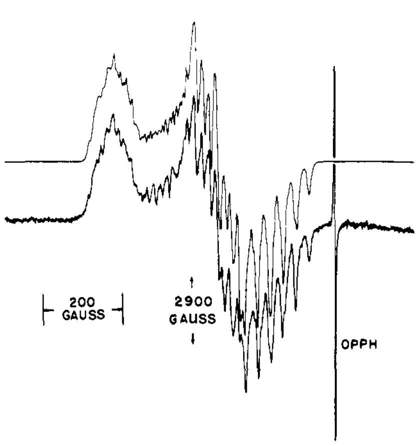

Figure 5. X-Band (9.1 GHz) EPR spectrum of a nickel-doped powder of $(Ph_3P)_2CuBr{\cdot}0.5C_6H_6$. Upper curve is computer simulated; lower is experimental.

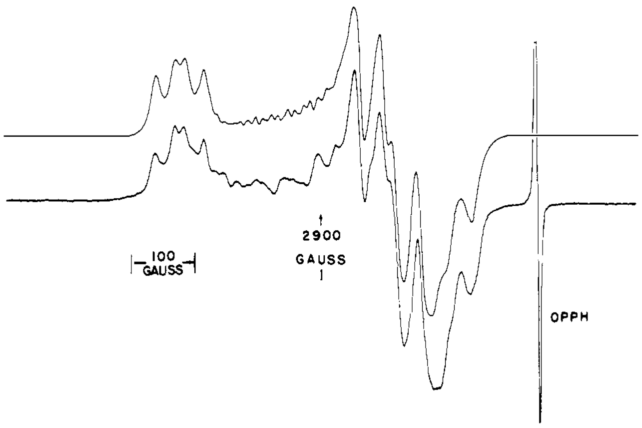

Figure 6. X-Band (9.1 GHz) EPR spectrum of a nickel-doped powder of $(Ph_3P)_2CuCl \cdot 0.5C_6H_6$. Upper curve is computer simulated; lower is experimental.

can be inferred from simple theoretical considerations. The nuclear quadrupole moments for both ^{79}Br and ^{81}Br are positive. Accordingly, thinking of the bromide ion as having some electron density withdrawn by the σ bond to nickel, one expects the largest electric field gradient, eq_1, to be positive and directed along the nickel-bromine bond. Thus, QD $(eQeq_1/4)$ should also be positive.

Although EPR-determined ligand quadrupole coupling constants have rarely been reported for paramagnetic transition metal complexes, NQR-determined quadrupole coupling constants have been reported for many diamagnetic complexes. If the asymmetry parameter, QE, is zero (it is usually small and in our case could be taken to be zero within experimental error), the NQR frequency, ν, is related to QD by the relationship, $\nu = 2QD$. Our value for QD, $+8.6 \times 10^{-4}$ cm^{-1}, would correspond to $\nu = 51$ MHz.

Farlee and Brown[20] have kindly searched for the bromine NQR resonances for our host material, $(Ph_3P)_2CuBr \cdot 0.5C_6H_6$. They found only one resonance at 65.90 MHz, which tentatively can be assigned to ^{79}Br, the isotope with the larger quadrupole moment (i.e., the larger transition intensity). Since Cu(I) has a complete d shell, the bromine NQR frequency can be directly related to the ionic character of the metal-halogen bond.[21] Proceeding along lines similar to Kubo et al.[21] we obtain an ~80% ionic character for the copper-bromine bond. Our value of ν for the nickel complex, which is comparable to that for the analogous copper complex, indicates that the nickel-bromine bond is also fairly ionic; the small reduction in ν is attributable to the presence of partly filled metal d orbitals suitable for metal-halogen π-back-bonding.[21]

Bromine Superhyperfine Coupling. The small positive isotropic shf coupling constant of 3×10^{-4} cm^{-1} corresponds to a nearly zero net s-orbital spin density, consistent with the idea that the nickel-bromine bond is fairly ionic.[16] Clearly, the unpaired electron is not involved in a substantial σ bond to the bromide ion. The resultant anisotropic shf coupling tensor (all in units of 10^{-4} cm^{-1}) is as follows: $B_1 = -10$, $B_2 = +28$, and $B_3 = -17$. The fact that this tensor is fairly axial about axis 2 indicates that the unpaired spin interacts with the bromine nucleus primarily through π-back-bonding involving the nickel d_{xy} orbital and the in-plane bromine p orbital perpendicular to the nickel-bromine bond. (That is, two lobes of the d_{xy} orbital point roughly toward the phosphorus ligands, while the two other lobes straddle the bromine ion.)

Electronic Zeeman Tensor. The orbital contributions to the g values are larger (i.e., cause larger g shifts) than for most cupric complexes because of the smaller charge on the metal atom (i.e., smaller crystal field splittings) in spite of a smaller spin-orbit coupling for Ni(I).[22] Since $g_{\parallel}(g_3)$ is considerably larger than $g_{\perp}$ (g_1 and g_2), the unpaired spin must be localized in an in-plane d_{δ} orbital. The above picture describing the nature of the anisotropic bromine shf coupling is consistent with the idea that the ground state orbital containing the unpaired spin is mainly d_{xy}, although the low symmetry (C_s) of the complex allows the ground-state orbital to have some $d_{x^2-y^2}$ and d_{z^2} content. In addition, the two excited-state d_{π} orbitals, d_{xz} and d_{yz}, will mix into the ground state via spin-orbit coupling.

The asymmetry and directions of the in-plane g components are a result of not only the energies and orientations of the two d_{π} orbitals but also the admixture of the d_{z^2} and $d_{x^2-y^2}$ orbitals allowed by the low symmetry of the complexes.[23] Thus, one cannot directly attribute the noticeable increase in the in-plane g anisotropy on going from the chloro to the bromo complex to the expected changes in the π system. Nevertheless, the fact that the in-plane g axes lie between the lobes of the ground-state orbital suggests that the d_{π} orbitals are primarily responsible for the in-plane g anisotropy.[23a]

Phosphorus Superhyperfine Coupling. The marked inequivalence of the two phosphorus shf tensors for both the chloro and bromo complexes was most unexpected. The shf anisotropies as well as their isotropic shf coupling constants are quite different. For the one phosphorus atom the shf tensor is nearly isotropic, while for the other phosphorus, it is axial. In addition, this inequivalency is noticeably greater for the bromide complex than the chloride complex. These facts suggest that as the metal-halogen bond becomes more covalent and includes more π-back-bonding, the two phosphorus-metal bonds differ more with respect to π-back-bonding. This idea would also fit the above suggestions of a strong metal-ligand π-system.

However, this inequivalency could arise from steric factors present in the crystal. The crystal structure of the copper host shows that the two copper-phosphorus bond lengths are slightly different and the two halogen-copper-phosphorus angles are moderately different. It is uncertain whether this small inequivalency is imposed by the host upon the guest or whether, indeed, a more severe inequivalency is characteristic of the isolated nickel complex. An x-ray diffraction determination of the structure of the corresponding undiluted Ni(I) complex would be interesting in this connection, but we have as yet not grown suitable single crystals.

Frozen Solutions. General features of the spectra of frozen solutions of the chloro- and the bromotris(triphenylphosphine)nickel(I) complexes matched with those of the analogous powdered dilute crystals. Accordingly, we infer that the main species in solution is the bis complex. However, not enough shfs could be clearly resolved in the spectra of frozen solutions to reveal whether the two phosphorus shf tensors were inequivalent in the solutions. Our observation that the amount of resolvable shfs was very dependent on the solvent mixture could indicate that other species are also present in solution.

Acknowledgment. We are grateful for research support provided by the donors of the Petroleum Research Fund, administered by the American Chemical Society, by the Research Corporation, and by the National Science Foundation. M.J.N. is grateful for a Proctor and Gamble predoctoral fellowship. We thank Dr. Tina Northern whose computer programs formed the core of the programs used in simulating spectra.

References and Notes

(1) Author to whom correspondence should be addressed.

(2) A review of the known nickel(I) complexes is given in A. N. Williamson, Ph.D. Thesis, University of Illinois, 1976.

(3) P. Heimbach, *Angew. Chem., Int. Ed. Engl.*, **3**, 648 (1964).
(4) (a) L. Porri, M. C. Gallazzi, and G. Vitulli, *Chem. Commun.*, 228 (1967); (b)

L. Porri, G. Vitulli, and M. C. Gallazzi, *Angew. Chem., Int. Ed. Engl.*, **6**, 452 (1967).
(5) M. L. H. Green and M. J. Smith, *J. Chem. Soc. A*, 639 (1971).
(6) C. S. Cundy and H. Noth, *J. Organomet. Chem.*, **30**, 135 (1971).
(7) S. Otsuka, A. Nakamura, T. Yoshida, M. Naruto, and K. Ataka, *J. Am. Chem. Soc.*, **95**, 3180 (1973).
(8) M. F. Lappert and G. Speir, *J. Organomet. Chem.*, **80**, 329 (1974).
(9) D. G. Holah, A. N. Hughes, B. C. Hui, and K. Wright, *Can. J. Chem.*, **52**, 2990 (1974).
(10) G. Vitulli, P. Pertici, C. Agami, and L. Porri, *J. Organomet. Chem.*, **84**, 399 (1974).
(11) E. Bartsch, E. Dinjus, and E. Uhlig, *Z. Chem.*, **15**, 317 (1975).
(12) K. Kanai, *J. Chem. Soc., Chem. Commun.*, 203 (1972).
(13) The latter situation is almost certainly the case. Studies in our laboratories strongly suggest that a nickel hydride is involved in the olefin isomerization. M. J. D'Aniello, Jr., Ph.D. Thesis, University of Illinois, 1976.
(14) R. A. Schunn, *Inorg. Chem.*, **15**, 208 (1976).
(15) M. J. D'Aniello, Jr., unpublished results.
(16) P. H. Davis, R. L. Belford, and I. C. Paul, *Inorg. Chem.*, **12**, 213 (1973).
(17) (a) L. K. White and R. L. Belford, *Chem. Phys. Lett.*, **37**, 553 (1976); (b) H. V. Van Willigen and J. G. M. Van Rens, *ibid.*, **2**, 283 (1968).
(18) D. Shaltiel and W. Low, *Phys. Rev.*, **124**, 1062 (1961).
(19) R. M. Golding, *Trans. Faraday Soc.*, **59**, 1513 (1963).
(20) R. Farlee and T. L. Brown, unpublished results, Department of Chemistry, University of Illinois, Urbana, Illinois.
(21) M. Kubo and D. Nakamura, *Adv. Inorg. Chem. Radiochem.*, **8**, 257 (1966).
(22) W. Hayes and J. Wilkens, *Proc. R. Soc. London, Part A*, **155**, 629 (1964).
(23) (a) M. A. Hitchman, C. D. Olson, and R. L. Belford, *J. Chem. Phys.*, **50**, 1195 (1968); (b) R. L. Belford, B. Harrowfield, and J. R. Pilbrow, to be submitted for publication.

The Experimental Charge Distribution in Sulfur Containing Molecules. Analysis of Cyclic Octasulfur at 300 and 100 K

P. Coppens,*[1a] Y. W. Yang,[1a] R. H. Blessing,[1a]
W. F. Cooper,[1a] and F. K. Larsen[1b]

Contribution from the Chemistry Department, State University of New York at Buffalo, Buffalo, New York 14214, and Department of Chemistry, Aarhus University DK8000, Aarhus, Denmark.

Received June 7, 1976

Abstract: X-ray and neutron diffraction measurements on cyclooctasulfur have been analyzed as part of a series of charge density analyses of sulfur containing molecules. The x-ray data (at 300 and 100 K) and the combination of x-ray and neutron data indicate a contraction of the atomic density at about 0.6 Å from the nucleus compared with the isolated spherical sulfur atom. Difference density at the midpoint of the S–S bond is about 0.05 e Å^{-3}, which is considerably lower than observed in diffraction studies of bonds between carbon and nitrogen atoms. Evidence is obtained for the directional character of the sulfur lone pair orbitals. An orbital exponent refinement of both room and low temperature x-ray data gives a best experimental single ζ value of 1.99 a_0^{-1} for the M shell orbitals assuming unperturbed K and L shells. Observed bond lengths and angles are in agreement with earlier, less precise, measurements.

Until recently charge density studies by diffraction methods have been concerned largely with development of methods. However, many computational procedures have now been developed and experimental errors have been reduced and are better understood. As a result experimental information on the charge distribution in crystals is becoming available and it is now feasible to study a number of related systems and thus concentrate on the chemical significance of the results.[2]

This report represents the first of a series of charge density studies of small sulfur containing molecules. Orthorhombic elemental sulfur was selected as a logical first choice, because knowledge of the charge distribution in monatomic sulfur may facilitate subsequent studies of more complex sulfur containing compounds.

Many organic and inorganic sulfur compounds are quite suitable for charge density analysis. Though the sulfur atom has more core electrons than carbon, nitrogen, and oxygen atoms, it is not so heavy that it is beyond the reach of x-ray charge density measurements.[3] There are a number of outstanding issues of chemical significance. It is usually assumed that sp hybridization is less important in sulfur than in first-row elements, a view supported by calculations of overlap integrals.[4] The question of participation of d orbitals is more controversial. The general lowering of theoretical energies when d functions are included has been attributed to limitations in the basis-set composition,[5] yet a consistent explanation[6] of the bonding in the "cage" compound S_4N_4 invokes the use of d orbitals to explain the short "across the ring" S···S distances of 2.58 and 2.69 Å found by Sharma and Donohue.[7] The most striking feature of the sulfur–sulfur interaction is the wide range of S–S distances from 1.99 Å in 4-phenyl-1,2-dithiolium cyanate[8] to 2.36–2.6 Å in thiathiaphtenes,[9] 2.58 and 2.69 Å in S_4N_4,[7] 2.98 Å in $S_4(NH)_4$,[10] to 3.33 Å in the across the ring "bond" in the present study of cyclooctasulfur. Also noteworthy are the 2.79 Å S . . . S *intra*chain and 3.48 Å *inter*chain interactions[11] in the polymeric low temperature superconductor $(SN)_x$. Short distances are also found in the triangular arrangement of the disulfide group and chloride ion in substituted dithiolium chlorides.[8]

Of further interest is the bonding between sulfur and nitrogen. The planarity of the S(NH)S group in $S_4(NH)_4$ and similar compounds[10] implies a partial double bond character, that must be absent in the "saturated" S–N system in the NH_3SO_3 zwitterion sulfamic acid.[12] ESCA measurements indicate that the SN bond in sulfur nitrogen ions[5b] is very polar, and a theoretical analysis of S_4N_4 suggests that the SN bonds[14] are bent much like the bent bonds in organic small ring compounds that have been observed in experimental charge density studies.[15]

The crystal structure of cyclooctasulfur at room temperature was studied by x-ray film techniques by Abrahams and collaborators.[16] The detailed analysis of the data during the period 1956–1965 has been reviewed by Donohue.[17] For the present study, room temperature x-ray and neutron, and low temperature (100 K) x-ray diffractometer data are used. Among further studies are an x-ray and neutron low temperature in-